Journal of CO2 Utilization 45 (2021) 101410

Contents lists available at ScienceDirect

Journal of CO2 Utilization

journal homepage: www.elsevier.com/locate/jcou

# The biogas-oxyfuel process as a carbon source for power-to-fuel synthesis: Enhancing availability while reducing separation effort

Felix Schorn [a,b,*], Dennis Lohse [a], Remzi Can Samsun [a], Ralf Peters [a], Detlef Stolten [b,c]

[a] Institute of Electrochemical Process Engineering (IEK-14), Forschungszentrum Jülich GmbH, 52428, Jülich, Germany
[b] Chair for Fuel Cells, RWTH Aachen University, 52072, Aachen, Germany
[c] Institute of Techno-Economic Systems Analysis (IEK-3), Forschungszentrum Jülich GmbH, 52428, Jülich, Germany

ARTICLE INFO

*Keywords:*
Power-to-fuel
Renewable methanol
Oxyfuel combustion
Biogenic $CO_2$ utilization
Biogas conversion
Techno-economic assessment

ABSTRACT

Producing synthetic fuels via Power-to-Fuel processes requires hydrogen and a carbon source. To attain a sustainable fuel, both reactants must originate from a renewable source. For the carbon source, biogas plants offer substantial potential. Hence, this paper presents a new biogas-oxyfuel process that couples a biogas plant with Power-to-Fuel production and enables a decentralized and economical supply of biogenic carbon dioxide for the production of renewable methanol. By using the oxygen byproduct of the Power-to-Fuel synthesis in the oxyfuel combustion of a combined heat and power unit, a simple separation of the $CO_2$ in the flue gas is made possible. To analyze the thermodynamic changes within the combustion engine when switching from regular to oxyfuel combustion, an AspenPlus model of the combined heat and power unit of a biogas plant is built up herein. Due to the higher heat capacity of the new working gas carbon dioxide in comparison to nitrogen, the ideal Otto engine cycle's mechanical efficiency drops by 5.8 percentage point. This drop in efficiency leads to a loss in revenue for the operator of the biogas plant. Together with the additional equipment expenditures for the $CO_2$ separation, this loss is defined as the $CO_2$ separation costs. For a retrofit of existing biogas plants with an installed electric power of 75−1000 kW, the $CO_2$ separation costs are determined to be 88−33 €/t. The process shown therefore offers a promising way to deliver biogenic $CO_2$ at low cost for decentralized Power-to-Fuel systems.

## 1. Introduction

Within the energy and transport sectors, the transition towards renewable electricity generation and the electrification of drivetrains will be two key strategies to lower dependency on fossil fuels and therefore reduce the greenhouse gas emissions. However, some modes of transportation, for example aviation, maritime and heavy-duty will to at least a certain extent still rely on liquid energy carriers with high volumetric energy density. Therefore, Schemme et al. [1] identified Power-to-Fuel (PtF) as a key to sustainable transport systems. Within this concept, electric energy (power) is transformed into fuel via the production of hydrogen in an electrolysis step and a subsequent reaction step with a carbon source to hydrocarbons, alcohols or ethers. One prominent example of this is methanol synthesis, which is comparably simple, already commercially-available for the reactants of $H_2$ and $CO_2$ and is therefore at a high technology readiness level (TRL) [2,3]. Methanol itself can be used as a fuel or transformed into a wide range of hydrocarbons, ethers or higher alcohols [4]. As can be seen from Eq. 1, two reactants are needed for the production of methanol:

$$3H_2 + CO_2 \rightarrow CH_3OH + H_2O \quad (1)$$

On the one side is hydrogen and on the other is carbon dioxide. To fulfill the requirement of being a renewable fuel, it is essential that both reactants are derived from a renewable source. As mentioned, for hydrogen this can be achieved through the electrolytic splitting of water powered by renewable electricity. Proton exchange and alkaline electrolyzers are already commercially available in the MW range [5]. For carbon dioxide, the question of whether the source is renewable is not as straightforward. A general overview about possible $CO_2$ sources for Power-to-Fuel applications, namely industry flue gases, air and biogenic sources, can be found in Hänggi et al. [6].

As $CO_2$ can be captured in large quantities from different industrial sectors and capture methods are commercially-available, these sources were amongst the first to be considered for Power-to-Fuel applications. Recent examples are the ALLIGN CCUS [7] and MefCO$_2$ [8] projects. However, nearly all of $CO_2$ emissions produced by industry are derived

* Corresponding author at: Institute of Electrochemical Process Engineering (IEK-14), Forschungszentrum Jülich GmbH, 52425, Jülich, Germany.
*E-mail address:* f.schorn@fz-juelich.de (F. Schorn).

https://doi.org/10.1016/j.jcou.2020.101410
Received 27 August 2020; Received in revised form 26 November 2020; Accepted 13 December 2020
Available online 6 January 2021
2212-9820/© 2021 The Authors. Published by Elsevier Ltd. This is an open access article under the CC BY license (http://creativecommons.org/licenses/by/4.0/).

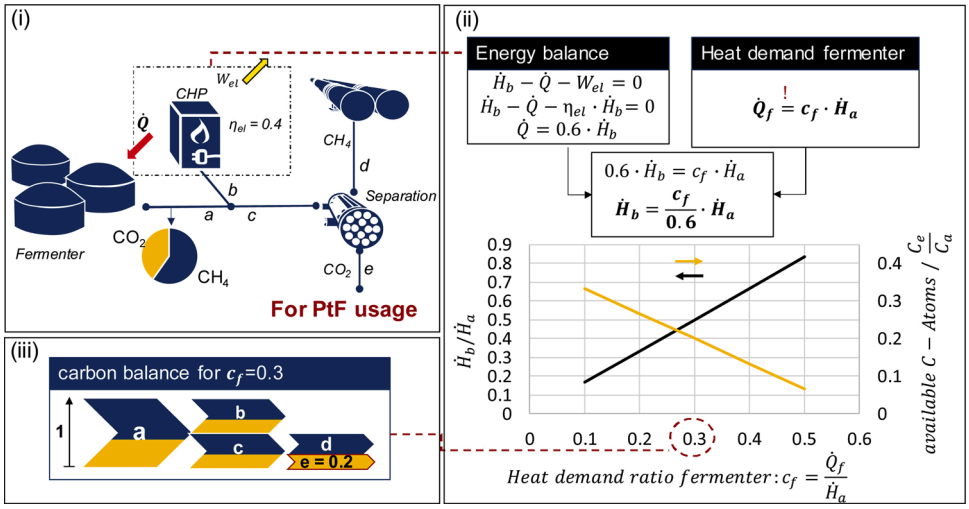


**Fig. 1.** State-of-the-art biogas separation for Power-to-Fuel usage: (i) biogas upgrading plant flowsheet; (ii) energy balance for the CHP with the resulting ratio of enthalpy stream b to a and available C-atoms for power-to-fuel usage depending on the heat demand ratio; (iii) graphical carbon balance for $c_f$=0.3.

from the combustion of fossil energy carriers, which will be significantly reduced in order to achieve the necessary greenhouse gas emissions reductions and hence will not be as readily available in the future. Furthermore, using $CO_2$ captured from fossil energy generation for the production of synthetic fuels would contradict the entire principle of generating a renewable fuel. In the worst case scenario, this approach would even justify the extended operation of facilities using fossil feedstocks. Therefore, only the process-related and unavoidable $CO_2$ emissions, as they partially occur alongside cement and steel production, could be seen as suitable Power-to-Fuel reactants. Here, a double use of $CO_2$ would at least reduce overall emissions.

The second source of $CO_2$ for Power-to-Fuel applications is the direct capture of $CO_2$ from the air (DAC: direct air capture) [9]. Several companies and research associations have developed various techniques to efficiently ad- or absorb carbon dioxide from the atmosphere [10]. Pilot plants and a first commercial plant have been built recently [11]. The use of the separated $CO_2$ in Power-to-Fuel systems is investigated, for instance, in the SOLETAIR project [12,13] and is foreseen for the planned Nordic Blue Crude plant in Norway [14]. The main advantage of this concept is that the supply of $CO_2$ is location-independent and can therefore be supplied where renewable electricity can be generated at low cost. This is especially important for the Power-to-Fuel technology, as it depends on inexpensive hydrogen. This is shown in Schemme et al. [15], where the $H_2$ cost was determined to be responsible for 58–83 % of the total production cost of synthetic fuels. The drawback of the DAC technology is that the energy demand is higher than, for example, the capture of $CO_2$ from flue gas [16]. To ensure carbon-neutral $CO_2$ production, the energy consumed within the recovery would have to originate from a renewable source as well.

The third $CO_2$ source for a possible PtF application are biogenic $CO_2$ emissions. Here, the production of ethanol via fermentation and of biogas are the main routes. In Europe and foremost in Germany, biogas production is a well-developed technology with a high degree of distribution [17]. Biogas contains between 30−50 vol. % of $CO_2$, the remaining 50−70 vol. % being methane [18]. Approximately 17,000 biogas plants are operated in Europe with over 10,000 running in Germany [19]. For Germany, Billig et al. [20] determined the amount of $CO_2$ within biogas to be 12 Mt/a, which would be a significant source for synthetic fuel production. $CO_2$ from biogas plants has already been analyzed or used in further reactions. Angelidaki et al. [18] examined several biogas upgrading technologies using hydrogen to enhance the methane yield, thus also coupling electrolysis systems with biogas plants in so-called Power-to-Gas processes. Two general possibilities are discussed: $CO_2$ can be either separated from biogas and chemically-reacted in the Sabbatier reaction to form methane or biologically-transformed into methane via hydrogen supply into the liquid phase of the biogas fermenter. Several pilot plants for Power-to-Gas applications are in operation [21], of which some use biogas as the $CO_2$ source. One example is the AUDI Power-to-Gas synthetic methane plant in Werlte, Germany, which uses $CO_2$ extracted from biogas and hydrogen from an electrolysis unit to produce synthetic methane [22]. On the side of liquid instead of gaseous synthetic fuel production, Marchese et al. [23] proposed a Power-to-Liquid system that coupled a biogas upgrading plant with an electrolysis unit and Fischer-Tropsch synthesis.

The significant biogenic $CO_2$ potential from biogas plants is distributed amongst the already mentioned large amount of biogas sites in Europe. In order to harness this potential, $CO_2$ must be separated from the biogas. This is currently performed in 216 biogas upgrading plants out of 10,000 total biogas sites in Germany [24], which are in average larger than the biogas plants without upgrading [25]. The recovered methane is fed into the natural gas grid, whereas the separated $CO_2$ is released into the atmosphere and could instead be accessible for Power-to-Fuel usage. The separation is performed using the established technologies of amine or water pressure washing, membrane processes or pressure swing absorption [18]. The small number of biogas upgrading plants, in contrast to the total amount of biogas sites, has an economic rationale. The average electric power of a biogas plant in Germany is 500 kW [25], which translates into a biogas flow of 208 $Nm^3/h$ if a mechanical efficiency of 0.4 for the combined heat and power unit (CHP) [26] and the volumetric energy content of a typical biogas of 6 $kWh/Nm^3$ [27] are assumed. Sahota et al. [28] report on a minimum capacity of biogas-upgrading plants of 200 $Nm^3/h$, below which biogas-upgrading plants cannot be economically operated. The reason for this behavior is the significant economy of scale effects between biogas capacities of 250–500 $Nm^3/h$ on the investment costs for biogas upgrading technologies reported in Beil and Beyrich [29] and Bauer et al. [30]. An average biogas plant is therefore too small for an economically-viable biogas upgrading operation. This leads to the observation that the $CO_2$ from the majority of biogas plants is not directly accessible for Power-to-Fuel applications and the biogas is therefore burnt in a CHP to generate electricity and heat. The question that therefore arises is: Can the significant but highly distributed carbon potential of biogas plants be made available in an economical manner for Power-to-Fuel applications?

To answer this question, the analysis in Fig. 1 shows the status quo of a biogas upgrade plant which, under the current state-of-the-art, would be necessary to provide carbon dioxide in the biogas for PtF usage. Fig. 1 (i) depicts a typical scheme of a biogas plant with a subsequent

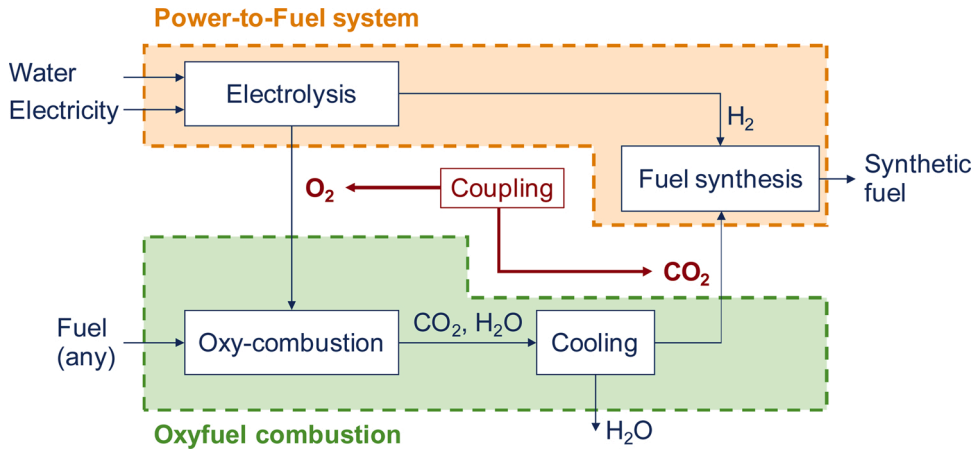


**Fig. 2.** Coupling of Power-to-Fuel systems with oxyfuel combustion.

separation of $CH_4$ and $CO_2$. After leaving the fermenter, the biogas (a) is split into two streams, (b) and (c). Stream (b) is sent to a CHP to supply the necessary heat for the fermenter and produce electricity for the local grid. Stream (c) is separated into methane (d) and carbon dioxide (e), which would then be accessible for Power-to-Fuel applications. According to the central coordinating agency in the area of renewable resources in Germany (FNR) [27], a typical ratio $c_f$ of the heat demand for a fermenter $\dot{Q}_f$ to the total energy of the produced biogas ($\dot{H}_a$) is about 0.3. Furthermore, a typical mechanical efficiency for a biogas CHP is approximately 0.4 [26]. If we take these numbers and place them in the energy balance around the CHP given in Fig. 1(ii), the results show that the biogas flow (c) going to the separation is significantly reduced to only 50 % of the original biogas flow (a) from the fermenter. This behavior is shown for varying heat demand ratios $c_f$ in the graph of Fig. 1(ii). On the left axis, the enthalpy ratio of stream (b) to (a) is given. With rising $c_f$ from 0.1 to 0.5, the amount of biogas that must be burnt in the CHP increases from 17 to 83 % of the total biogas produced. On the right axis, the resulting quantity of carbon atoms for possible PtF applications is given in orange. Here, not only the $CO_2$, but also the carbon within the methane, is considered. Depending on the heat demand of the fermenter, only 7–33 % of the produced biogenic carbon atoms would be accessible for Power-to-Fuel usage. This is also shown in Fig. 1(iii). Of the total amount of carbon in the biogas (1), only 20 % (e = 0.2) is available for possible PtF application for the typical heat demand ratio of 30 % of the fermenter's enthalpy flow.

This evaluation shows that a typical biogas separation plant, apart from the aforementioned minimum size limitation, is not an optimal carbon source for a PtF application, as the maximum yield of biogenic carbon is only about 33 %. This is reasonable, as within the process presented in Fig. 1, the desired products are heat, electricity and methane. However, if the aims were re-defined as exploiting the full carbon potential of the biogas and still being able to produce heat and electricity, a complete combustion of biogas in a CHP with a downstream separation of $CO_2$ would be necessary. Given that every methane molecule reacts to a carbon dioxide molecule during combustion, the volumetric quantity of biogenic $CO_2$ for PtF usage per plant would approximately double. This is already done in the large majority of the noted 10,000 biogas plants in Germany. The problem with a regular combustion process in a CHP is that the produced $CO_2$ is highly diluted by the nitrogen in the air. A stoichiometric combustion of a biogas containing 50 % methane would lead to an exhaust gas with a volumetric $CO_2$ content of approximately 25.8 % (2 / 7.762); see Eq. 2.

$$CH_4 + CO_2 + 2(O_2 + \frac{79}{21}N_2) \rightarrow 2CO_2 + 2H_2O + 3.762\ N_2 \quad (2)$$

To capture the carbon dioxide from the flue gas, the complex technology of flue gas separation would be necessary, which would again not be economically-viable.

The dilution of the flue gas with nitrogen can be avoided by means of an oxyfuel combustion. Here, the fuel is combusted with pure oxygen, leaving only a flue gas mixture containing water, $CO_2$ and potential incombustible pollutants [31]. The oxyfuel combustion with further separation of the $CO_2$ was already investigated for power plants [32] and the production of cement [33]. In such applications, oxygen is supplied through an air separation unit. Since in a Power-to-Fuel system, oxygen is a byproduct of water electrolysis, the coupling of oxyfuel combustion in a biogas plant and a Power-to-Fuel application can be beneficial. This concept is qualitatively shown in Fig. 2. The coupling of the similar Power-to-Gas technology with an oxyfuel combustion of natural gas for electric grid balancing is discussed by Bailera et al. [34]. To the best knowledge of the authors, a system analysis of a biogas plant, coupled with a Power-to-Fuel system to enable an oxyfuel combustion and a simple separation of the $CO_2$ has not been investigated thus far. For this purpose, a system will be investigated as shown Fig. 2 with the focus on the oxyfuel combustion of biogas. Therefore, the aim of the present work is to analyze the retrofit of existing biogas plants to an oxyfuel operation. Here, the mass balances, thermodynamic changes within the system and the economic impact of such a retrofit will be analyzed. This concept enables then a biogenic carbon dioxide supply for decentralized Power-to-Fuel systems or other carbon dioxide use cases.

## 2. Methodology and approach

As is presented in the introduction, the overall goal of this study was to answer the question as to whether the significant but highly distributed quantity of biogenic $CO_2$ emissions can be made accessible in an economical fashion for Power-to-Fuel applications. This question will be answered by outlining the principle, characteristics and economics of a biogas-oxyfuel process. The process can either be used to retrofit already existing biogas plants or for new ones to use the easily available carbon dioxide in synthetic fuel production. The focus of this paper lays on the retrofit of already existing biogas plants. The following chapter will explain the methodology and approaches used. After highlighting the overall flow chart of the process, the modeling approach followed will be presented. This includes the implementation of the thermodynamic conditions of a four-stroke gasoline engine with the help of process engineering software, the subsequent adaptation to a fuel gas consisting of biogas, oxygen and $CO_2$ and the separation of $CO_2$ out of the flue gas of the oxyfuel process. For the economic evaluation, the principle and assumptions are described at the end of this section.

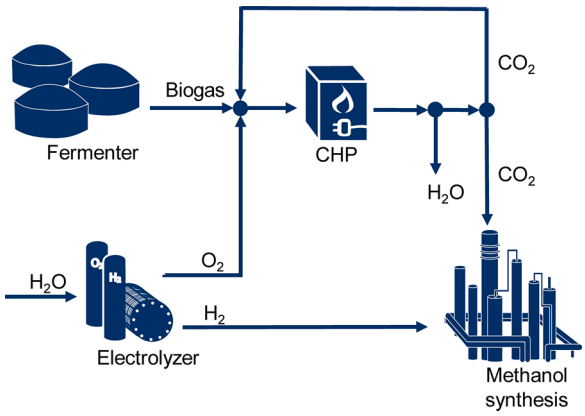


**Fig. 3.** Scheme of the biogas-oxyfuel process.

### 2.1. Process flow sheet of the developed biogas-oxyfuel process

Fig. 3 shows the general scheme of the developed biogas-oxyfuel process. Within the electrolyzer, water is split into oxygen and hydrogen by means of renewable electricity. Hydrogen is sent for methanol synthesis while the oxygen byproduct is sent to the combined heat and power plant where it is mixed with biogas from the fermenter as well as recycled and cooled $CO_2$. The recycled $CO_2$ takes over the role of the inert gas, which is usually $N_2$ when combusting with air. The exhaust gas from the CHP is cooled down in a condenser to partially dry the flue gas. The resulting $CO_2$ stream is split into two streams, which are guided to the methanol synthesis and exhaust gas recirculation (EGR) segments.

Looking at the scheme, a couple of questions arise, namely:

1 Overall mass balance: How much methanol can be produced from a given amount of biogas? Is sufficient oxygen produced as a byproduct of electrolysis to run the oxyfuel process?
2 How is the maximum temperature in the CHP controlled? What are the additional differences in the combustion thermodynamics of using $CO_2$ instead of $N_2$ as an inert gas?

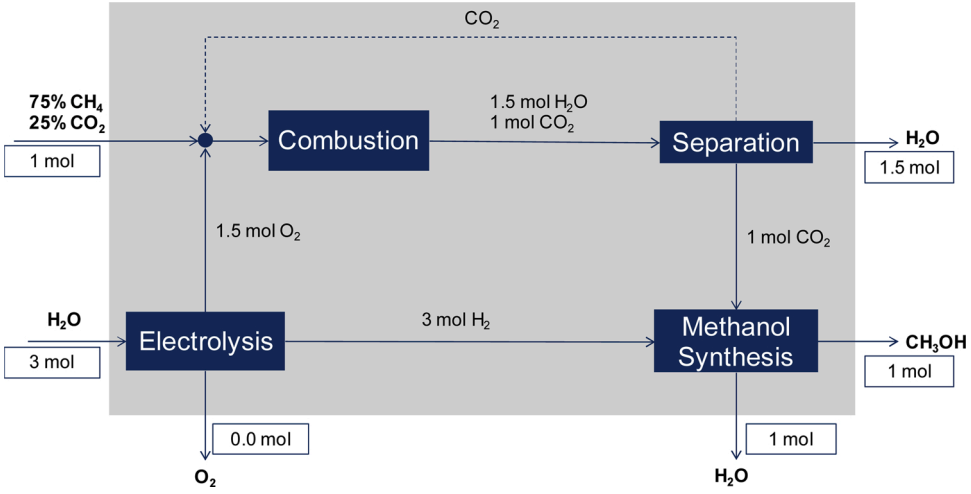


**Fig. 4.** Molar balance for the maximum methane content of biogas of 75 vol.%.

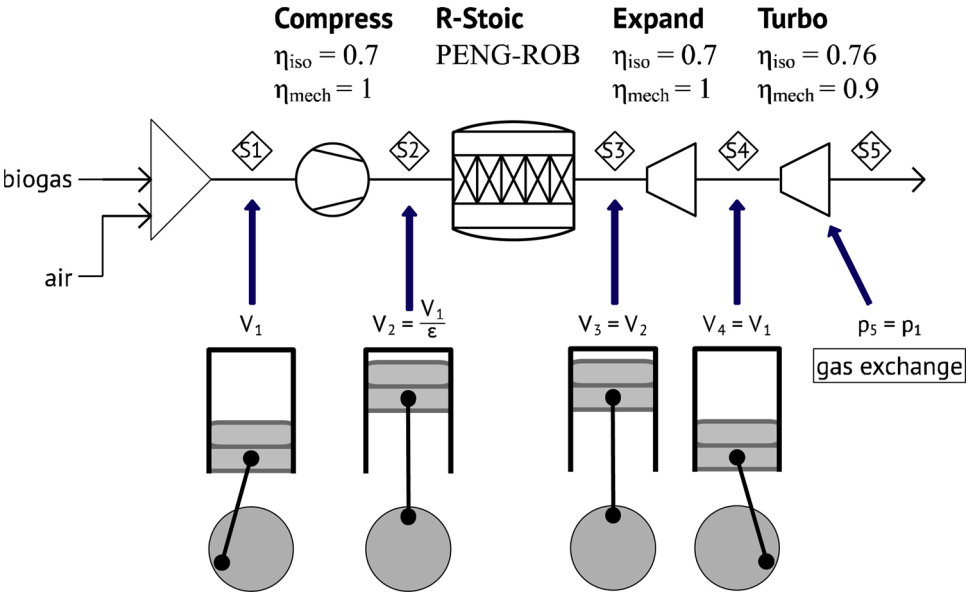


**Fig. 5.** Transfer of the four-stroke Otto cycle in process engineering software.

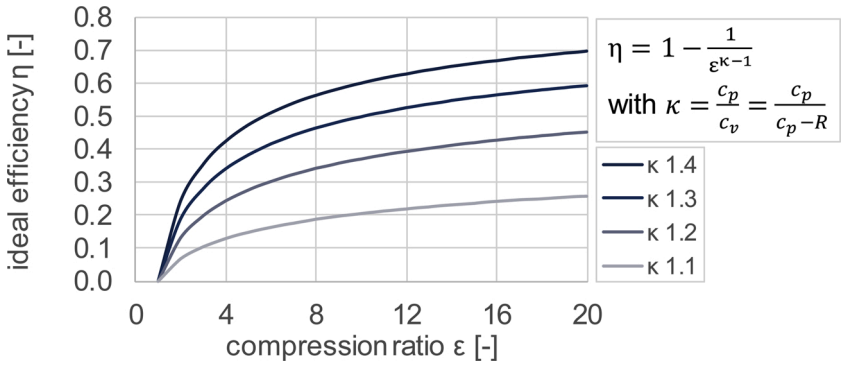


**Fig. 6.** Dependency of the ideal efficiency of an Otto engine on the isentropic coefficient κ over the compression ratio ε.

To answer the first question, Eq. 2 shows the general stoichiometric combustion equation for 1 mol of biogas with a variable amount of $CH_4$ of $0 > \chi_{CH_4} < 1$:

$$\chi_{CH_4} \cdot CH_4 + (1 - \chi_{CH_4}) \cdot CO_2 + 2 \cdot \chi_{CH_4} \cdot O_2 \rightarrow 1 \cdot CO_2 + 2 \cdot \chi_{CH_4} \cdot H_2O \quad (3)$$

One key result of this equation is that the amount of $CO_2$ per mole of biogas is independent of the share of methane in the biogas, as every mole of methane reacts to one mole of $CO_2$. This also results in the conclusion that one mole of methanol can be produced per mole of biogas; see Eq. 1. However, to convert one mole of $CO_2$ into one mole of methanol, 3 mol of hydrogen are needed. With the production of 3 mol of hydrogen during electrolysis, 1.5 mol of oxygen are produced as a side product:

$$3H_2O \rightarrow 3H_2 + 1.5O_2 \quad (4)$$

Therefore, the maximum share of methane within biogas in the oxyfuel production of methanol can be:

$$1.5 \cdot O_2 = 2 \cdot \chi_{CH_{4,max}} \cdot O_2 \rightarrow \chi_{CH_{4,max}} = 0.75 \quad (5)$$

As biogas seldom exceeds a methane content of 75 vol.% [35], it can be stated that the oxygen produced in the electrolysis exceeds the oxygen demand for the oxyfuel combustion. Fig. 4 shows the molar balance for the maximum methane content of 75 vol.% in the biogas. For any concentration with less than 75 vol.% methane, surplus oxygen will be produced by the electrolysis unit.

To answer the second question, the thermodynamic states of the combustion process must be assessed. This was done by setting up a process model that will be introduced in the following section.

### 2.2. Process modelling of the cogeneration unit

To analyze the key thermodynamic states within the CHP, two processes were modelled using the process engineering software, AspenPlus. First, a base process was set up to transfer a regular four-stroke Otto cycle, which a CHP uses, in a steady-state process engineering simulation by evaluating the thermodynamic conditions for each of the following steps: adiabatic compression, isochoric combustion, adiabatic expansion and the gas exchange. The principle with the chosen efficiencies [36], assumptions and thermodynamic models is shown in Fig. 5. Second, the base model was further adapted to the oxyfuel combustion process. For this purpose, air was replaced by pure oxygen and recycled $CO_2$ from the flue gas.

#### 2.2.1. Base model

For the base model, the four transitions from one step to the other of the Otto cycle shown in Fig. 5 are modelled in AspenPlus using the Peng-Robinson equation of state model [37,38] in the following way:

1→2 The compression of the intake gas mixture is modelled as an adiabatic compression (Compr) with an isentropic efficiency of 70 % [36]. With a defined compression ratio ε, the pressure at stage 2 ($p_2$) is calculated with a design specification. It varies $p_2$ so that the following constraint is met:

$$\varepsilon = \frac{V_1}{V_2} = \frac{\rho_2}{\rho_1} \; with \; m_1 = m_2 \quad (6)$$

2→3 The second step is modelled as an adiabatic reactor with isochoric combustion (RStoic). As the mass and volume remain constant in this step, the density will also not change. Therefore, the pressure can be calculated by adapting the reaction pressure to fulfill the requirement $\rho_3 = \rho_2$..

3→4 The adiabatic expansion (Compr) is modelled with the condition that the densities of step 1 and 4 are equal, as are the mass and volume. The isentropic efficiency is again 70 %. The final pressure $p_4$ is calculated by fulfilling design specification $\rho_4 = \rho_1$.

4→5 To model the gas exchange with a steady-state process engineering software, the remaining pressure $p_4$ in the cylinder is expanded in a turbine (Compr) to atmospheric pressure. This agglomerates the two-step exhaust discharge and fresh mixture intake. As the atmospheric pressure is constant, no further design specification must be added. The turbocharger is modeled with an isentropic efficiency of 76 % and a mechanical efficiency of 90 % [36].

The total mechanical energy of the model is the sum of the mechanical work of the piston compressor (1), expansion within the piston (3) and gas turbine (4):

$$P_{mech} = P_{comp} + P_{expand} + P_{turbo} \quad (7)$$

A design specification is implemented to adjust the biogas flow to the desired total mechanical energy. With the total mechanical energy of the CHP, the mechanical efficiency of the system can be calculated with the incoming mass flow and lower heating value of methane $LHV_{CH4}$ = 50.048 MJ/kg [39] as:

$$\eta_{mech} = \frac{P_{mech}}{\dot{m}_{CH_4} \cdot LHV_{CH_4}} \quad (8)$$

It is obvious that the approach used and process engineering software has limits and implies some simplifications compared to the actual process within a four-stroke spark-ignited engine. Nevertheless, the described model delivers sufficient information for a first evaluation of the process. The overall goal of the base model is to calculate the three characteristic values of maximum pressure and temperature, as well as the efficiency of the CHP. This important input data is used for the switch from regular biogas to oxyfuel combustion. The comparison and validation for maximum pressure and the efficiency will be performed using the literature data [26,40,41] in the results section.

#### 2.2.2. Oxyfuel combustion

For the oxyfuel combustion process, the same model as described was used, but the ambient air was replaced by a mixture of pure oxygen from the electrolysis and $CO_2$ from the recycle stream. A design

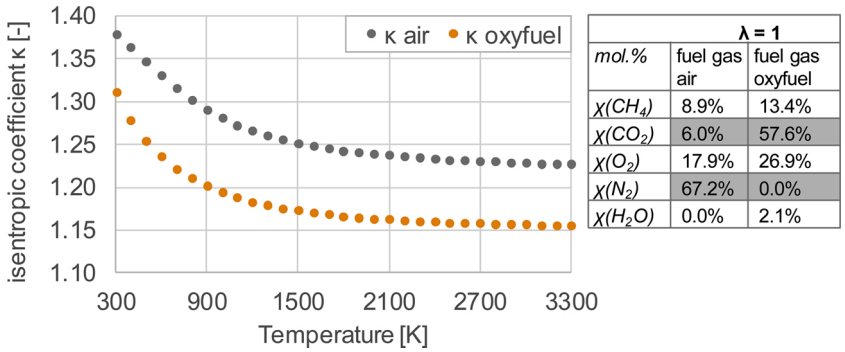


| | λ = 1 | |
|---|---|---|
| mol.% | fuel gas air | fuel gas oxyfuel |
| $\chi(CH_4)$ | 8.9% | 13.4% |
| $\chi(CO_2)$ | 6.0% | 57.6% |
| $\chi(O_2)$ | 17.9% | 26.9% |
| $\chi(N_2)$ | 67.2% | 0.0% |
| $\chi(H_2O)$ | 0.0% | 2.1% |

**Fig. 7.** Temperature-dependency of isentropic coefficients for air and oxyfuel mixtures with biogas.

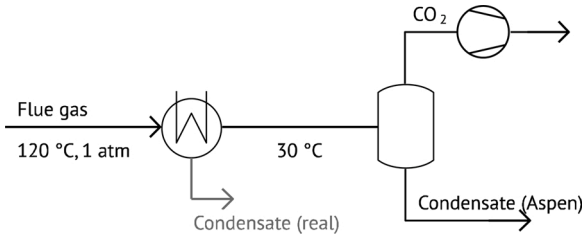


**Fig. 8.** $CO_2$ separation system implemented in AspenPlus: Flash evaporator implemented to analyze carbon slip through the condensate. In reality, the condensate would be separated in the heat exchanger.

specification controls the amount of oxygen entering the combustion chamber to fulfill the requirement of stoichiometric combustion ($\lambda = 1$). To ensure that the engine faces neither thermal nor mechanical overload, the maximum temperature and pressure, as well as the efficiency from the base case, are used as limits. To control the thermal load, a design specification adds enough $CO_2$ that the maximum temperature of the regular combustion with air is not exceeded. A mechanical overload would occur if either the maximum pressure or efficiency were to increase compared to the base model. If the hardware of the CHP is not changed (i.e., the compression ratio ε), the thermodynamic analysis shows that due to the change in the working gas from air to oxygen/$CO_2$, the efficiency of the engine will drop slightly: The efficiency of an ideal Otto engine depends on the compression ratio and isentropic coefficient κ, which is depicted in Fig. 6.

To investigate the isentropic coefficient of the oxyfuel fuel gas, the specific heat capacities under constant pressure were calculated for a temperature window from 300 to 3300 K using the UNIFAC model using the property analysis of AspenPlus. Fig. 7 shows that over the full temperature window, the resulting isentropic coefficient of the oxyfuel mixture with biogas is lower than the mixture with air. The shown compositions are for a stoichiometric combustion. The amount of $CO_2$ in the oxyfuel fuel gas is already adapted to fulfill the requirement of a constant maximum temperature compared to the base process with air. Meanwhile, the isentropic coefficient is lower for the oxyfuel due to the higher heat capacity of $CO_2$ compared to air. Hence, a drop in efficiency will occur when operating the CHP under the same boundary conditions and therefore the mechanical overload can be neglected. However, the reduced efficiency will lead to a lower amount of electricity produced for a given biogas flow rate and result in a loss of revenue for the operator of the plant. This difference in income will be assigned to the produced $CO_2$ and, together with the investment cost for further equipment, will determine the $CO_2$ cost of the proposed oxyfuel plant. The economic assessment will be described in detail in chapter 2.3.

The thermodynamic analysis conducted here shows that a retrofit of existing biogas plants to the oxyfuel combustion process is feasible but is accompanied by reduced efficiency if the engine is not adapted. If this process were built up in a new biogas plant, an adapted engine (i.e., compression ratio, valve timing, intercooling system, water injection, etc.) could compensate the reduced efficiency due to the higher heat capacity of the $CO_2$. In this regard, the theoretical approach performed represents a worst-case consideration without optimization of the engine.

### 2.2.3. $CO_2$ separation

The flue gas produced by the oxyfuel process consists of carbon dioxide and water. After the combustion, it is cooled down to deliver process heat. The product specification of CHP manufacturers state a flue gas temperature of 120 °C and atmospheric pressure after the process heat utilization [42], which will be taken as inlet parameters. The separation system of the products is shown in Fig. 8. It is modeled with a shell and tube heat exchanger (HeatX), a flash evaporation (Flash2) and fan (Compr) with isentropic and mechanical efficiencies of 0.75 and 0.95 respectively to overcome the pressure losses. The output of this separation model is the required heat transfer area, the power of the fan and the $CO_2$ slip out of the system through the condensate.

The flash evaporator is only used as a theoretical unit to evaluate the $CO_2$ slip of the system through the outgoing condensate due to the dissolution of $CO_2$ in water. It will not be installed in reality though and therefore not considered in the economic assessment. In the later separation unit, the heat exchanger has a separate outlet for gas and condensate. $CO_2$ dissolution can be analyzed by implementing the equations of the dissociation of water (Eq. 9), the reaction of water with carbon dioxide to hydrogen carbonate (Eq. 10) and the dissociation of hydrogen carbonate to a carbonate ion (Eq. 11) [43]. For this assessment, the Electrolyte NRTL model in AspenPlus was used:

$$2H_2O \leftrightarrow OH^- + H_3O^+ \tag{9}$$

$$2H_2O + CO_2 \leftrightarrow HCO_3^- + H_3O^+ \tag{10}$$

$$H_2O + HCO_3^- \leftrightarrow CO_3^{2-} + H_3O^+ \tag{11}$$

The respective equilibrium constants can be calculated by means of Eq. 12:

$$\ln(K_{eq}) = A + \frac{B}{T} + C \cdot \ln(T) + D \cdot T \tag{12}$$

using the equilibrium constants from Arachchige and Melaaen [43].

### 2.3. Economic assessment

Within this evaluation, a retrofit of existing biogas plants to a biogas-oxyfuel operation is considered. The biogas plants already include a fermenter, a biogas pretreatment for moisture and sulfur removal and a cogeneration unit and already operate economically in their present form. In this case, as discussed in the previous section, a drop in efficiency and therefore reduced electricity production will occur, which leads to a loss in revenue for the operator of the biogas plant. Additionally, further investments for the newly installed units, heat

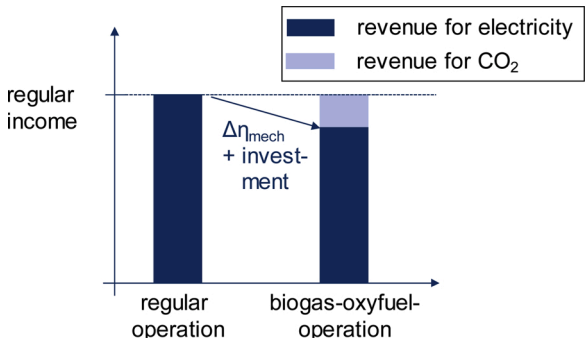


**Fig. 9.** Reduced income when operating the biogas-oxyfuel process is compensated by revenue for $CO_2$.

exchanger and fan have to be made. To balance out the loss in revenue and additional capital cost, the operator of the plant would need to be refunded for the generated $CO_2$. Otherwise the assumed retrofit would not be made by the operator, since it would only result in increased costs. This is independent on the further use of the generated $CO_2$, whether it would be in Power-to-Fuel applications or for example carbon capture and storage. Therefore, the additional investment costs and the loss in revenue are assigned to the produced $CO_2$, which is depicted in Fig. 9. As a Power-to-Fuel plant, consisting of an electrolyzer and methanol synthesis system, as depicted in Fig. 3, is considered to be installed at the same location, the side product oxygen is assumed free of charge. The economic assessment of the Power-to-Fuel plant is not part of this publication. The necessary $CO_2$ costs for a continuous economic operation are calculated with the following economic assessment.

The loss in revenue (LIR) depends on the feed-in tariff for the electricity production $t_{el}$, the flow rate $\dot{V}_{biogas}$, the lower heating value $e_{biogas}$ of the biogas and the difference in the electric efficiency $\Delta\eta$ of the CHP. Therefore, the LIR can be expressed as:

$$\dot{LIR} = t_{el} \cdot \dot{V}_{biogas} \cdot e_{biogas} \cdot \Delta\eta \tag{13}$$

To allocate this loss in revenue to the produced mass of $CO_2$, the $CO_2$-specific LIR can be expressed as:

$$\frac{LIR}{m_{CO_2}} = t_{el} \cdot \frac{e_{biogas} \cdot \Delta\eta}{\rho_{CO_2}} \text{ with } \dot{m}_{CO_2} = \dot{V}_{biogas} \cdot \rho_{CO_2} \tag{14}$$

This specific loss in revenue will be treated as a cost of utility $c_{UT}$ within the further techno-economic assessment. To reach the described break-even point, the cost of manufacturing (COM) of $CO_2$ must be equal to the amount of $CO_2$ produced multiplied by the revenue it recoups ($r_{CO_2}$):

$$COM = m_{CO_2} \cdot r_{CO_2} \rightarrow r_{CO_2} = \frac{COM}{m_{CO_2}} \tag{15}$$

The additional cost for the capital investment and operation of the heat exchanger and fan can be calculated with the cost estimation method for the chemical processes of Turton et al. [44]. Here, the fixed capital investment (FCI) is determined with an equipment cost-based method. Based on the initial cost for standard equipment defined in Turton et al. [44], factors that consider the building year (2018 in this publication), material, pressure and total direct and indirect plant costs are multiplied. Finally, the cost of manufacturing of a product without depreciation ($COM_d$) is then given as:

$$COM_d = 0.180\ FCI + 2.73 C_{OL} + 1.23(C_{UT} + C_{WT} + C_{RM}) \tag{16}$$

The operating labor $C_{OL}$ is neglected in this economic assessment, as it is assumed that the required heat exchanger and fan will be maintained by the same staff that runs the biogas and CHP plant and will therefore not lead to additional labor costs. The costs for waste treatment $C_{WT}$ and those for distribution, sales and research and development

**Table 1**
Key assumptions for capital and operation cost estimations for the retrofit of the proposed system to existing biogas plants.

| Capital cost estimations | | Operation cost estimations | |
|---|---|---|---|
| Specification | Value | Specification | Value |
| Additional equipment | Heat exchanger, fan | Cost of oxygen | 0 €/t |
| Investment cost estimation method | Turton et al. [44] | Cost of electricity (for $C_{fan}$) | 0.15 €/kWh |
| Depreciation method | Annuity | Feed-in tariff $t_{el}$ | 0–0.3 €/kWh |
| Interest rate | 7% | $C_{OL}$ | 0 |
| Lifetime | 20 a | $C_{WT}$ | 0 |
| Reference year | 2018 | $C_{RM}$ | 0 |

$C_{RM}$ can be neglected in this case of a very small "chemical plant". For the depreciation, the annuity method with an interest rate $i = 7\%$, a lifetime $n = 20\ a$ and no working capital is assumed. This leads to the reduced equation for the cost of manufacturing (COM) of the produced $CO_2$ [45]:

$$COM = 0.141\ FCI + 1.03 \cdot C_{UT} + FCI \cdot \frac{i \cdot (1+i)^n}{(1+i)^n - 1} \tag{17}$$

The utility costs consist of the described loss in revenue (LIR) and the electricity costs for running the fan $C_{fan}$. By dividing Eq. 17 by the $CO_2$ produced by the biogas oxyfuel process and considering Eq. 14 and Eq. 15, the specific break-even revenue for the $CO_2$ can be calculated as:

$$r_{CO_2}\left[\frac{€}{t_{CO_2}}\right] = 1.03 \cdot \left(t_{el} \cdot \frac{e_{biogas} \cdot \Delta\eta}{\rho_{CO_2}} + \frac{C_{fan}}{m_{CO_2}}\right) + \frac{FCI}{m_{CO_2}} \cdot \left(0.141 + \frac{i \cdot (1+i)^n}{(1+i)^n - 1}\right) \tag{18}$$

The first term represents the additional operating expenditures (OPEX) and the second term the annual capital costs (ACC) imposed by the depreciation of the capital expenditures (CAPEX) for the required additional equipment. Any $CO_2$ revenue higher than this value will constitute an additional profit for the plant operator. To summarize the methodology of the economic assessment, Table 1 shows the key assumptions used to determine the capital and operational expenditures.

## 3. Results

This section will highlight, on the one hand, the simulation results of the implemented process modeling of the biogas-oxyfuel process. After presenting the outcome and characteristic parameters of the base model, the results will be transferred to the oxyfuel and separation model. The system will be laid out for biogas plants with an initial electric output of 75–1000 kW, as 500 kW of installed capacity is the average for biogas plants without upgrading in Germany [25]. On the other hand, the results of the oxyfuel combustion and $CO_2$-separation model will act as the input data for the economic assessment of the newly developed plant. The break-even cost for the produced $CO_2$ to run the biogas with the same revenue as prior to the retrofit will then be calculated and analyzed for the different sizes of the system.

### 3.1. Base model

Fig. 10 shows the resulting flow diagram for the calculated pressures and temperatures of the system. A biogas containing 60 vol.% $CH_4$ and 40 vol.% $CO_2$ was assumed and the compression ratio was set to $\varepsilon = 13$, which is a typical value for CHP engines [26]. The maximum temperature and pressure reach 2407 °C and 122 bar, respectively, and the observed maximum pressure lies within the regular range of natural gas engines for power generation [40]. The maximum temperature for adiabatic combustion serves as a theoretical value for comparison with the oxyfuel combustion in order to avoid a thermal overload.

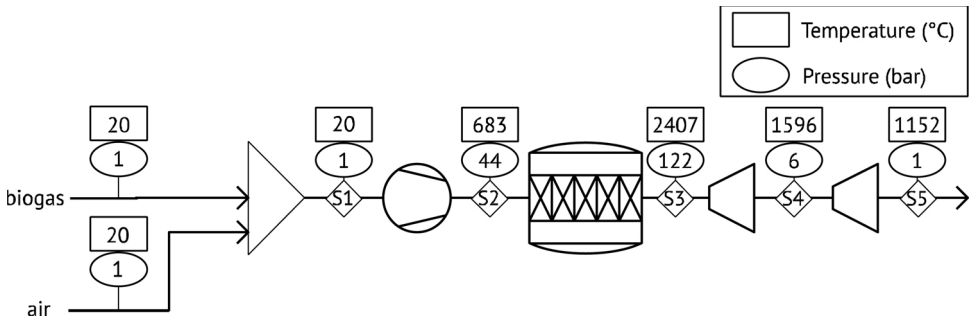


**Fig. 10.** Simulation results of the base model.

**Table 2**
Stream results of the investigated biogas plant sizes.

| Biogas plant electric output [kW] (Eq. 7) | Biogas flow [kmol/h] | Biogas enthalpy flow [kJ/s] | $CO_2$ flow in combustion chamber [kmol/h] | $CO_2$ flow in flue gas [kmol/h] | $CO_2$ flow in flue gas [kg/h] |
|---|---|---|---|---|---|
| 75 | 1.39 | 186 | 0.55 | 1.39 | 61 |
| 125 | 2.30 | 308 | 0.92 | 2.30 | 101 |
| 250 | 4.60 | 614 | 1.84 | 4.60 | 203 |
| 375 | 6.88 | 919 | 2.75 | 6.88 | 302 |
| 500 | 9.21 | 1,231 | 3.68 | 9.21 | 405 |
| 1000 | 18.44 | 24,645 | 7.38 | 18.44 | 811 |

The mass or molar flows of the system are not depicted in Fig. 10, as they do not affect the pressure or temperature of the ideal system and are therefore independent transfer information for the oxyfuel combustion model. However, the respective biogas flow into the system for the different system sizes is needed for the $CO_2$ separation model to calculate the investment cost for the additional equipment. Table 2 shows the investigated biogas plant sizes and gives the results for the biogas molar and enthalpy flows, as well as the $CO_2$ molar flows. The mean value for mechanical efficiency according to Eq. 7 is 40.6 %, which corresponds well to current natural gas engines for power generation from biogas in cogeneration plants [26]. As is stated in Eq. 3, the molar flow of $CO_2$ in the flue gas is identical with that of biogas and independent of the $CO_2$ concentration in the biogas. The resulting $CO_2$ molar flow will not change when transferring to the oxyfuel combustion model, but will be far easier to separate from the flue gas and be available for a Power-to-Fuel application.

### 3.2. Oxyfuel combustion model

For the oxyfuel combustion, the maximum temperature of the base model was used as the reference to which to adjust the recycled $CO_2$ content in the flue gas of the CHP. The results are shown in Fig. 11. To limit the temperature to 2407 °C, the $CO_2/CH_4$ mass ratio must be set to 11.8. As a result, 68 % of the $CO_2$ in the flue gas must be recycled. The maximum pressure of 119 bar is below the 122 bar of the base model, which prevents a possible mechanical overload. Because of the greater heat capacity of the working gas, the temperature of stream S5 is higher than the base model. This will result in a higher heat output of the CHP plant. Due to the described differences in the thermodynamic properties

**Table 3**
Initial vs. oxyfuel electric output of the different biogas plant sizes. For each size, the biogas inlet flow is identical.

| Initial biogas plant electric output [kW] | Biogas electric output with oxyfuel combustion [kW] |
|---|---|
| 75 | 64 |
| 125 | 107 |
| 250 | 214 |
| 375 | 319 |
| 500 | 428 |
| 1000 | 857 |

**Table 4**
Stream composition of the oxyfuel combustion system (the streams are depicted in Fig. 11).

| Stream | Substance | Composition in mol.% |
|---|---|---|
| Biogas | $CH_4$ | 0.600 |
| | $CO_2$ | 0.400 |
| $O_2$ | $O_2$ | 1.000 |
| $CO_2$ | $CO_2$ | 0.960 |
| | $H_2O$ | 0.040 |
| S1 | $CO_2$ | 0.576 |
| | $O_2$ | 0.269 |
| | $H_2O$ | 0.021 |
| | $CH_4$ | 0.134 |
| S3 | $CO_2$ | 0.711 |
| | $O_2$ | 0.000 |
| | $H_2O$ | 0.289 |
| | $CH_4$ | 0.000 |

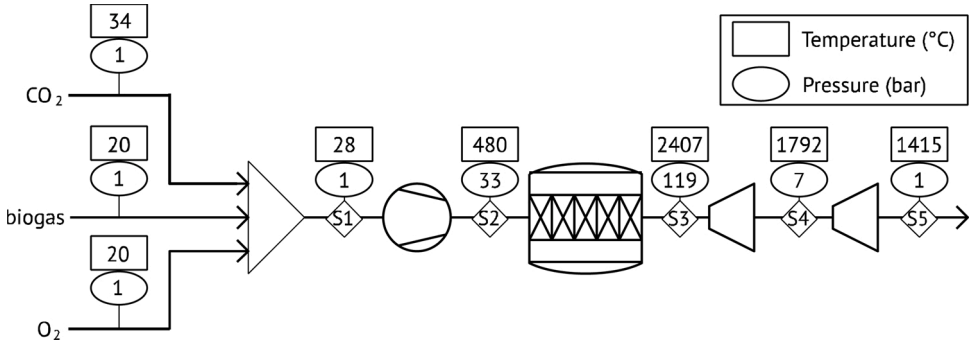


**Fig. 11.** Simulation results of the oxyfuel combustion system.

**Table 5**
Required heat transfer area for the $CO_2$ separation system.

| Initial Biogas plant electric output [kW] | A [$m^2$] |
|---|---|
| 75 | 8.4 |
| 125 | 14.4 |
| 250 | 25.4 |
| 375 | 40.4 |
| 500 | 49.0 |
| 1000 | 101.3 |

**Table 6**
Condensate composition in mol.-%.

| $H_2O$ | $CO_2$ | $H_3O^+$ | $HCO_3^-$ | $OH^-$ | $CO_3^-$ |
|---|---|---|---|---|---|
| 0.999 | 4.76e-6 | 2.01e-6 | 2.01e-06 | 2.39e-12 | 1.3e-12 |

of the working gases, the mechanical efficiency drops to 34.8 %, which translates into an absolute drop of $\Delta\eta = 5.8$ % pt. and a reduction in the mechanical power of approximately 14.5 %. Table 3 therefore compares the initial biogas plant electricity output of the new one with the oxyfuel combustion. Both processes have the same biogas inlet flow. For the subsequent discussion, the initial biogas plant electricity output will be used as a reference for the power class to describe the different system sizes.

Table 4 shows the stream compositions of the model according to Fig. 11. The inlet $CO_2$ is saturated with water at a temperature of 34 °C and is already a result of the $CO_2$ separation model discussed in the next section. As desired, stream three (S3), which leaves the combustion, only contains $CO_2$ and water.

### 3.3. $CO_2$ separation

The flue gas of the oxyfuel combustion model enters the $CO_2$ separation at 120 °C, as this is a typical temperature of flue gases after a process heat utilization as stated in the methodology section. Since a retrofit of an existing biogas plant is investigated in this publication, the heat extraction out of the flue gas is not modelled. Further, no thermal integration of the $CO_2$ separation system with the combustion model exists. From this temperature, the flue gas is cooled down further to 30 °C in a shell and tube heat exchanger, modeled in Aspen Plus. The regular cooling fluid is liquid water, which enters the heat exchanger at 25 °C. The outcome of the model is the required heat transfer areas for each power class, which are depicted in Table 5 and the resulting pressure drop of 61 mbar within the heat exchanger. The pressure drop is used in the calculations for the economic assessment of the operating costs. The mean heat transfer coefficient k was calculated to 237 W/$m^2$ K.

Additionally, the $CO_2$ slip through the condensing water was investigated in a flash evaporator. Here, Eq. 9 - Eq. 11 were implemented. The resulting composition of the condensate is shown in Table 6. The low amount of $CO_2$ in the water results in an overall $CO_2$ slip of only 0.018 %.

### 3.4. Economic assessment

Drawing on the results of the previous sections, the loss in revenue and the investment and operating costs of the additional equipment can be calculated. Fig. 12 shows the investment cost for the heat exchanger and fan. With the method of Turton et al. [44], the minimum and maximum capacities are defined for all equipment types. For the chosen shell and tube heat exchangers, the minimum heat transfer area is 10 $m^2$ and for fans, the minimum gas flow rate is 1 $m^3$/s. As all of the investigated system sizes have flow rates under the defined minimum, the investment costs for the fan are identical for all system sizes and represent the minimum available size within this cost prediction method. It is obvious that this will not be the case for real application. However, an extrapolation outside the minimum defined system sizes would not be in agreement with the approach defined by Turton et al. [44]. When comparing the investment cost in Fig. 12, on the left, the

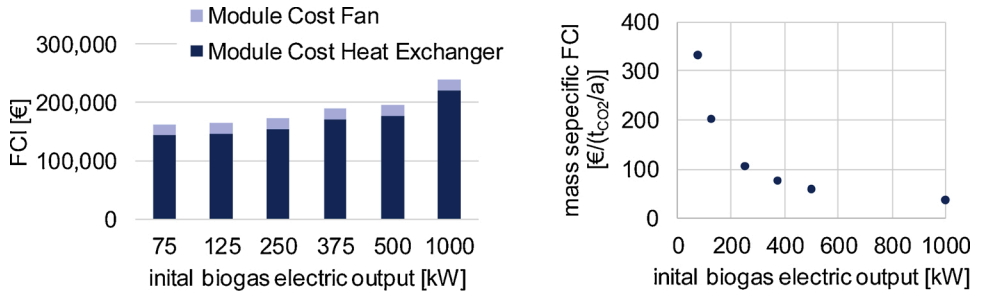


**Fig. 12.** Module costs for the additional equipment of the system (left); mass specific FCI depending on the biogas system size (right).

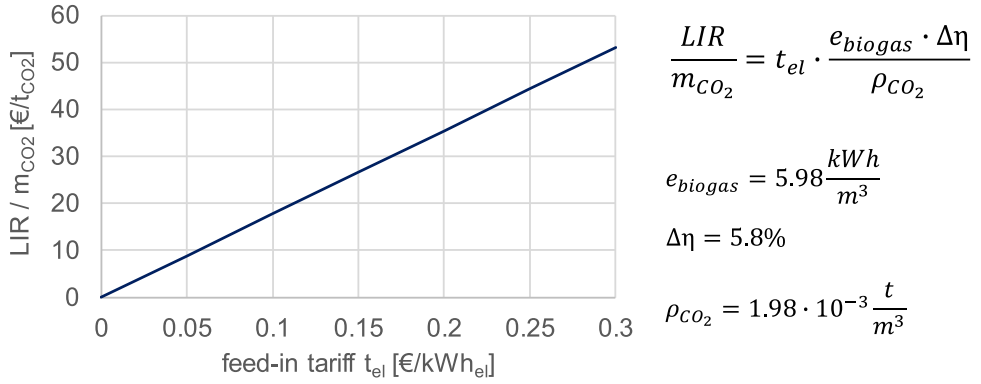


**Fig. 13.** Loss in revenue as a function of the feed-in tariff with the calculated drop in efficiency.

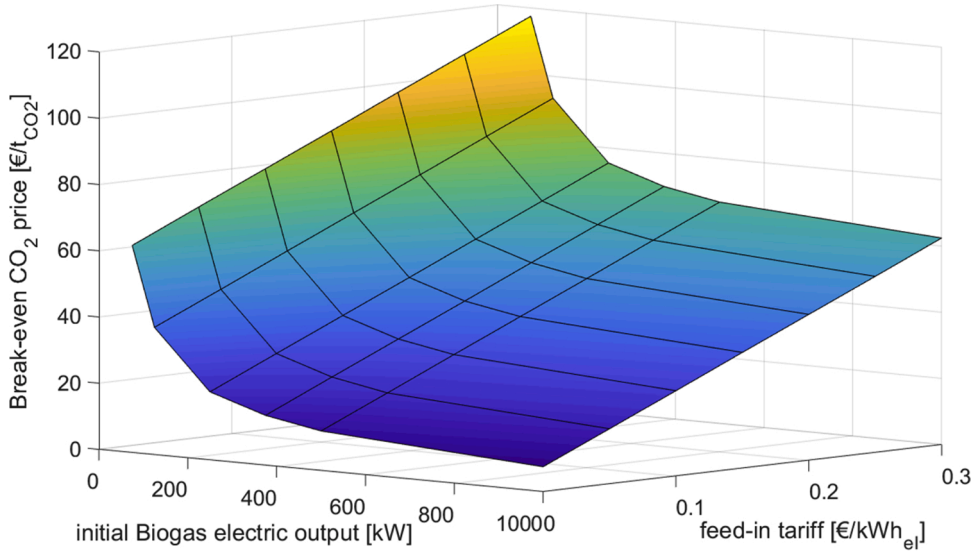


**Fig. 14.** Break-even $CO_2$ price as function of the system size and feed-in tariff for the electricity produced.

additional costs for the required system only increase slowly with the system size. This results in a sharp decrease in the investment costs over the yearly produced mass of $CO_2$, which is depicted on the right-hand side of Fig. 12. Therefore, in terms of capital investment costs, the proposed configuration will be especially beneficial for larger systems.

The loss in revenue in proportion to the produced $CO_2$ was specified in Eq. 14 and depends on the difference in the mechanical efficiency and feed-in tariff for the electricity produced. With the calculated drop in efficiency of $\Delta\eta = 5.8$ % pt., the loss in revenue becomes only linearly dependent on the feed-in tariff $t_{el}$ when switching from the regular to oxyfuel combustion, as depicted in Fig. 13. Between the typical compensation prices of 0.05 – 0.25 €/kWh, a $CO_2$ price of approximately 9–44 €/t would offset the loss in revenue from the lower mechanical efficiency of the combustion engine.

On the basis of the information gathered and Eq. 18, the break-even revenue cost can be calculated for the different system sizes:

$$r_{CO_2}\left[\frac{€}{t_{CO_2}}\right] = 1.03 \cdot \left(t_{el} \cdot \frac{e_{biogas} \cdot \Delta\eta}{\rho_{CO_2}} + \frac{C_{fan}}{m_{CO_2}}\right) + \frac{FCI}{m_{CO_2}} \cdot \left(0.141 + \frac{i \cdot (1+i)^n}{(1+i)^n - 1}\right) \quad (19)$$

The cost of the fan $C_{fan}$ is calculated with the specific power consumption (see Fig. A1) and an electricity price of 0.15 €/kWh. The results for the break-even $CO_2$ price $r_{CO_2}$ are shown in Fig. 14. The already observed trends in Figs. 12 and 13 are combined here, which means that the minimal break-even price for the produced $CO_2$ decreases for larger system sizes and increases for higher feed-in tariffs. It is notable that even for an unconventionally high compensation of 0.3 €/$kWh_{el}$ and the smallest biogas plant size, the resulting break-even $CO_2$ price does not surpass 120 €/t. This value represents the current $CO_2$ separation cost for large industrial flue gases with post-combustion techniques [46].

The feed-in tariff of 0 €/$kWh_{el}$ in Fig. 14 is only included for the sake of completeness, but does not represent a valid solution. The primary output of the biogas plant is still electricity and heat, as the oxyfuel process only allows a simple separation of the new product $CO_2$. If the operator is not compensated for the electrify produced (= 0 €/kWh), the plant will not run. As stated earlier, the chosen method assumes economical operation of the plant under the given feed-in tariff and calculates the required $CO_2$ compensation for the additional equipment and the loss in revenue due to the lower efficiency. For the combination of any system size and feed-in tariff, Fig. 14 shows a break-even price above which an additional profit for the operator will be generated.

For a typical feed-in tariff for German biogas plants built up to 2014 of 0.15 €/$kWh_{el}$, the detailed operating and capital costs are exemplarily shown in Table 7. As operational expenditures are predominantly dependent on the loss of revenue due to decreased mechanical efficiency, the higher electricity demand of the fan with increasing system size only has a marginal impact on the OPEX. The resulting $CO_2$ break-even prices of between 33–88 €/$t_{CO2}$ are again at the lower end of current $CO_2$ separation costs from flue gases.

Fig. 15 shows the composition of the $CO_2$ production costs in a pie chart for three different system sizes and the feed-in tariff of 0.15 €/kWh. For larger systems, the loss in revenue becomes the most relevant cost factor for the $CO_2$ produced via the oxyfuel system, for example with a 68 % share for a biogas plant in the 500 $kW_{el}$ power class. This offers significant cost reduction potentials for newly-built biogas plants with oxyfuel combustion technology given that, as mentioned earlier, the drop in efficiency might be far less for an adapted engine.

## 4. Discussion

Referring back to the overall scheme of the process presented in Fig. 3, this study showed the possibility of accessing the significant, but

**Table 7**
Cost composition of the break-even $CO_2$ price for a feed-in tariff of 0.15 €/kWh.

| Initial biogas plant electric output [kW] | OPEX (Fan + LIR) [€] | CAPEX [€] | $CO_2$ produced [t/a] | OPEX [€/$t_{CO2}$] | CAPEX [€/$t_{CO2}$] | $r_{CO_2}\left[\frac{€}{t_{CO_2}}\right]$ |
|---|---|---|---|---|---|---|
| 75 | 12,900 | 31,200 | 500 | 26 | 62 | 88 |
| 125 | 21,600 | 31,800 | 840 | 26 | 38 | 64 |
| 250 | 43,200 | 33,500 | 1680 | 26 | 20 | 46 |
| 375 | 64,700 | 36,400 | 2520 | 26 | 14 | 40 |
| 500 | 86,400 | 38,000 | 3360 | 26 | 11 | 37 |
| 1000 | 172,700 | 46,000 | 6720 | 26 | 7 | 33 |

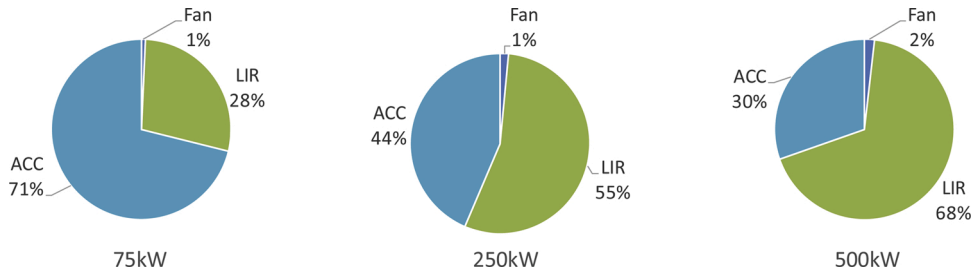


**Fig. 15.** Composition of the $CO_2$ production cost for three different system sizes [ACC: annual capital cost; LIR: loss in revenue].

**Table 8**
Annual $CO_2$ and possible methanol production from the BOP Process, together with the required hydrogen.

| Biogas plant electric output [kW] (Eq. 7) | $CO_2$ flow in flue gas [kg/h] | Annual $CO_2$ production [t/a] | Methanol production capacity [t/a] | $H_2$ required for methanol production [t/a] |
|---|---|---|---|---|
| 75 | 61 | 486 | 354 | 67 |
| 125 | 101 | 811 | 590 | 112 |
| 250 | 203 | 1621 | 1181 | 223 |
| 375 | 302 | 2416 | 1759 | 333 |
| 500 | 405 | 3243 | 2362 | 446 |
| 1000 | 811 | 6492 | 4728 | 894 |

highly distributed quantities of renewable $CO_2$ produced by biogas plants. Table 8 shows the annual $CO_2$ production of the analyzed system sizes with 8,000 operation hours, the producible methanol and required hydrogen. To produce one kilogram of methanol, 1.373 kg $CO_2$ and 0.189 kg of hydrogen are required [47]. It should be noted that the annual $CO_2$ production quantities of the systems are at their respective maximums. The classic approach of a separation into $CO_2$ and methane would only yield 7–33 % of the biogenic carbon, as shown in Fig. 1.

The system approach in this paper is based on a steady-state model, which operates with constant hydrogen and oxygen streams from an electrolysis unit. With the ongoing transition of the energy sector towards renewable and fluctuating electricity production, the possibility of dynamic operation of the system would be desirable. This could be achieved with either dynamic operation of the complete system or with the implementation of gas buffer storages. With the dynamic operation of the complete system, a fluctuating operation of the methanol synthesis running at pressures of up to 8 MPa and temperatures of 250 °C is challenging. Constant methanol production can be achieved with gas storage for biogas, $CO_2$, $H_2$ and $O_2$. With this configuration, the system could either draw electricity from the grid to produce hydrogen or supply electricity via the CHP. The resulting costs for the gas storage and especially the reduced operating hours would, however, affect the system's economics.

The proposed system varies strongly in two major points compared to the current state of the art presented in Fig. 1. First of all, in the proposed system, the whole biogenic carbon is made available for a Power-to-Fuel usage by combusting the entire biogas in a CHP while also producing electricity and heat. In contrast, for a state of the art biogas upgrading system, this amount only accumulated to roughly 20 % of the biogenic carbon for a typical heat demand of the fermenter. Secondly, the separation of $CO_2$ is also fundamentally different in the proposed system compared to the state of the art. While here, $CO_2$ is separated from a biogas to yield the desired product methane, in the proposed system $CO_2$ only has to be separated from water in the flue gas via condensation. This is achieved by combusting the biogas with oxygen and thereby reducing the separation complexity and energetic effort significantly. However, a comparison of the current state of the art biogas upgrading to the proposed system is not entirely fair, since current biogas upgrading systems are not laid out to produce a pure carbon dioxide stream, but are instead designed to produce methane for the gas grid. Therefore, the respective products of the two systems are different.

Compared to industrial post combustion techniques, the biogas-oxyfuel process yields similar prices with 33–88 €/$t_{CO2}$, even though the capture capacity with of maximal 6492 t/a (see Table 8) is significantly smaller than current industrial sequestration capacities of up to 8.4 Mt/a [48]. This can be explained by the simple extraction with a heat exchanger in the biogas-oxyfuel process, the possibility to use the combined heat and power unit also in an oxyfuel mode and the availability of oxygen from the electrolysis at no costs. If the oxygen would have to be generated onsite, the $CO_2$ price would rise accordingly.

Table 8 The environmental impact of this system was not assessed in detail in this publication and should be further studied. A life cycle assessment from Eggemann et al. [49] reported on significant environmental enhancements of a similar system concept compared to a fossil methanol production.

Biogas plants built in Germany through 2014 formerly received a guaranteed feed-in tariff for 20 years, depending on their size and the type of biomass they used [50]. However, since 2014, this funding has been rearranged, which resulted in a tender system in the current renewable energy law, EEG2017 [51]. This tendering protocol resulted in a sharp drop in installed biogas plants, as they were no longer economical [52]. An exception are small manure biogas plants with an installed capacity of up to 75 kW. These plants still receive a guaranteed compensation of 0.2314 €/kWh. However, if a biogas plant would no longer be capable of running economically, for example because of a reduced or expired federal guaranteed electricity compensation, the renewable product $CO_2$ could serve as new income to again achieve economical operation of the plant. To determine the required break-even cost for the $CO_2$ in this case would require a complete economic assessment of the biogas plant, which is not the focus of this paper.

## 5. Conclusion

As stated in the introduction, Power-to-Fuel processes are in need of a renewable $CO_2$ source, apart from the hydrogen produced by electrolysis. Biogas sources represent significant but not easily accessible potential. The introduced biogas-oxyfuel process offers a new way to make use of the full biogenic carbon potential for a Power-to-Fuel process by using the oxygen side-product of the electrolysis to run the CHP by means of oxyfuel combustion. Using pure oxygen yields an exhaust gas that contains only $CO_2$ and water, which drastically reduces the separation effort. To control the temperature within the engine, part of the separated $CO_2$ is recycled. An AspenPlus model was developed to analyze the differences between the regular combustion of biogas with air in comparison to oxyfuel combustion. Because of the higher heat capacity of carbon dioxide in comparison to nitrogen, the mechanical efficiency of the engine drops if a retrofit without engine adaptation is applied. This leads to a drop of $\Delta\eta = 5.8\%$ pt. of the ideal Otto engine cycle efficiency, having had an original efficiency of 40.6 %. The resulting loss in revenue for the electricity compensation and cost of the

additional heat exchanger and fan equipment varies between 88 – 33 €/t of separated $CO_2$ for a feed-in tariff of 0.15 €/$kWh_{el}$ and for system sizes of between 75–1000 kW of electricity production under normal conditions. Those production costs already lie within the range of the separation cost of fossil industrial flue gas separation. The discussed process is therefore already capable of delivering $CO_2$ at low cost for small systems, even for this worst-case scenario, with an engine that is not adapted to the new working gas. With growing installed capacity, the $CO_2$ production costs decrease and the share of the loss in revenue increases, which offers further cost reductions if the drop in mechanical efficiency is reduced by an adapted engine.

The coupling of Power-to-Fuel production with the oxyfuel combustion of biogas was found to be highly beneficial. The separation effort is reduced while the maximal biogenic carbon yield is made available. With this concept, even small biogenic $CO_2$ sources can be made available in an economical manner. However, this coupling makes both processes dependent on each other, meaning that one process cannot run without the other. A transfer of the concept of oxyfuel combustion with Power-to-Fuel systems to similar sites, where biogenic or unavoidable $CO_2$ emissions are emitted from combustion, could also be beneficial.

Overall, this study offers a sustainable option to supply $CO_2$ from biogenic sources for Power-to-Fuel applications at considerable cost. The research question raised at the beginning can be answered under the following circumstances: The highly distributed carbon potential of biogas plants can be made available in an economical manner for Power-to-Fuel applications through the biogas-oxyfuel process that was developed. The coupling criteria for this process is that the Power-to-Fuel plant is dimensioned to utilize the full gaseous biogenic carbon potential of its host biogas plant.

## CRediT authorship contribution statement

**Felix Schorn:** Conceptualization, Methodology, Software, Validation, Investigation, Visualization, Writing - original draft. **Dennis Lohse:** Methodology, Software, Investigation, Visualization, Writing - review & editing. **Remzi Can Samsun:** Conceptualization, Writing - review & editing, Supervision. **Ralf Peters:** Conceptualization, Writing - review & editing, Supervision, Funding acquisition. **Detlef Stolten:** Supervision, Funding acquisition.

## Declaration of Competing Interest

The authors declare that they have no known competing financial interests or personal relationships that could have appeared to influence the work reported in this paper.

## Appendix A

Fig. A1

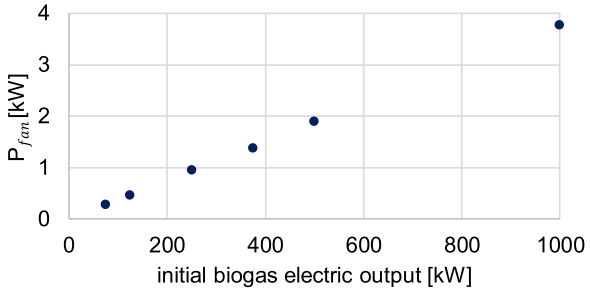


**Fig. A1.** Power consumption of the electric fan for the different system sizes.

## Appendix B. Supplementary data

Supplementary material related to this article can be found, in the online version, at doi:https://doi.org/10.1016/j.jcou.2020.101410.

## References

[1] S. Schemme, R.C. Samsun, R. Peters, D. Stolten, Power-to-fuel as a key to sustainable transport systems – an analysis of diesel fuels produced from $CO_2$ and renewable electricity, Fuel 205 (2017) 198–221, https://doi.org/10.1016/j.fuel.2017.05.061.
[2] D.S. Marlin, E. Sarron, O. Sigurbjornsson, Process advantages of direct $CO_2$ to methanol synthesis, Front. Chem. 6 (2018) 446. https://www.ncbi.nlm.nih.gov/pubmed/30320077.
[3] A. O'Connell, A. Konti, M. Padella, M. Prussi, L. Lonza, Advanced Alternative Fuels Technology Market Report 2018, EUR 29937 EN, European Commission, 2019, https://publications.jrc.ec.europa.eu/repository/handle/JRC118306.
[4] F. Schmidt, L. Reichelt, C. Pätzold, Catalysis of methanol conversion to hydrocarbons, in: M. Bertau (Ed.), Methanol: The Basic Chemical and Energy Feedstock of the Future, 2014, pp. 423–591.
[5] A. Buttler, H. Spliethoff, Current status of water electrolysis for energy storage, grid balancing and sector coupling via power-to-gas and power-to-liquids: a review, Renew. Sustain. Energy Rev. 82 (2018) 2440–2454, https://doi.org/10.1016/j.rser.2017.09.003.
[6] S. Hänggi, P. Elbert, T. Bütler, U. Cabalzar, S. Teske, C. Bach, C. Onder, A review of synthetic fuels for passenger vehicles, Energy Rep. 5 (2019) 555–569, https://doi.org/10.1016/j.egyr.2019.04.007.
[7] ALLIGN CCUS WP4 - CO2 Re-use, 2020 [Accessed 15.05.2020; https://www.alignccus.eu/about-project/work-package-4-co2-re-use-0].
[8] MefCO2- Project, 2020 [Accessed 15.05.2020; http://www.mefco2.eu/project_progress.php].
[9] A. Goeppert, M. Czaun, G.K. Surya Prakash, G.A. Olah, Air as the renewable carbon source of the future: an overview of CO2 capture from the atmosphere, Energy Environ. Sci. 5 (7) (2012) 7833, https://doi.org/10.1039/C2EE21586A.
[10] National Academies of Sciences, Engineering, Medicine, Negative Emissions Technologies and Reliable Sequestration: A Research Agenda, 2019, p. p. 510, https://doi.org/10.17226/25259.
[11] M. Fasihi, O. Efimova, C. Breyer, Techno-economic assessment of CO2 direct air capture plants, J. Clean. Prod. 224 (2019) 957–980, https://doi.org/10.1016/j.jclepro.2019.03.086.
[12] SOLETAIR, Power-to-Liquid: 200 Liters of Fuel From Solar Power and the Air's Carbon Dioxide, 2020 [Accessed 15.05.2020; https://www.kit.edu/kit/english/pi_2017_103_power-to-liquid-200-liters-of-fuel-from-solar-power-and-the-air-s-carbon-dioxide.php].
[13] F.V. Vázquez, J. Koponen, V. Ruuskanen, C. Bajamundi, A. Kosonen, P. Simell, J. Ahola, C. Frilund, J. Elfving, M. Reinikainen, N. Heikkinen, J. Kauppinen, P. Piermartini, Power-to-X technology using renewable electricity and carbon dioxide from ambient air: SOLETAIR proof-of-concept and improved process concept, J. Co2 Util. 28 (2018) 235–246, https://doi.org/10.1016/j.jcou.2018.09.026.
[14] Nordic Blue Crude, 2020 [Accessed 15.05.2020; https://nordicbluecrude.no/].
[15] S. Schemme, J.L. Breuer, M. Köller, S. Meschede, F. Walman, R.C. Samsun, R. Peters, D. stolten, H2 based synthetic fuels: a techno-economic comparison of alcohol, ether and hydrocarbon production, Int. J. Hydrogen Energy 45 (8) (2020) 5395–5414, https://doi.org/10.1016/j.ijhydene.2019.05.028.
[16] D. Krekel, R.C. Samsun, R. Peters, D. Stolten, The separation of CO 2 from ambient air – a techno-economic assessment, Appl. Energy 218 (2018) 361–381, https://doi.org/10.1016/j.apenergy.2018.02.144.
[17] N. Scarlat, J.-F. Dallemand, F. Fahl, Biogas: developments and perspectives in Europe, Renew. Energy 129 (2018) 457–472, https://doi.org/10.1016/j.renene.2018.03.006.
[18] I. Angelidaki, L. Treu, P. Tsapekos, G. Luo, S. Campanaro, H. Wenzel, P.G. Kougias, Biogas upgrading and utilization: current status and perspectives, Biotechnol. Adv. 36 (2) (2018) 452–466. https://www.ncbi.nlm.nih.gov/pubmed/29360505.
[19] M. Prussi, M. Padella, M. Conton, E.D. Postma, L. Lonza, Review of technologies for biomethane production and assessment of Eu transport share in 2030, J. Clean. Prod. 222 (2019) 565–572, https://doi.org/10.1016/j.jclepro.2019.02.271.
[20] E. Billig, M. Decker, W. Benzinger, F. Ketelsen, P. Pfeifer, R. Peters, D. Stolten, D. Thran, Non-fossil CO2 recycling-The technical potential for the present and future utilization for fuels in Germany, J. Co2 Util. 30 (2019) 130–141, https://doi.org/10.1016/j.jcou.2019.01.012.
[21] M. Thema, F. Bauer, M. Sterner, Power-to-gas: electrolysis and methanation status review, Renew. Sustain. Energy Rev. 112 (2019) 775–787, https://doi.org/10.1016/j.rser.2019.06.030.
[22] K. Ghaib, F.-Z. Ben-Fares, Power-to-Methane: a state-of-the-art review, Renew. Sustain. Energy Rev. 81 (2018) 433–446, https://doi.org/10.1016/j.rser.2017.08.004.
[23] M. Marchese, E. Giglio, M. Santarelli, A. Lanzini, Energy performance of Power-to-Liquid applications integrating biogas upgrading, reverse water gas shift, solid oxide electrolysis and Fischer-Tropsch technologies, Energy Conversion and Management: X 6 (2020), https://doi.org/10.1016/j.ecmx.2020.100041.
[24] Deutsche Energie-Agentur GmbH: Einspeiseatlas, 2019 [Accessed 01.09.2019; https://www.biogaspartner.de/einspeiseatlas/].

[25] J. Daniel-Gromke, N. Rensberg, V. Denysenko, W. Stinner, T. Schmalfuß, M. Scheftelowitz, M. Nelles, J. Liebetrau, Current developments in production and utilization of biogas and Biomethane in Germany, Chemie Ingenieur Technik 90 (1–2) (2018) 17–35, https://doi.org/10.1002/cite.201700077.
[26] M. Engines, MAN Gas Engines for Power Generation in Cogeneration Plants, 2019 [Accessed 03.09.2019; https://www.engines.man.eu/global/en/power/gas-power-generation/in-focus/E3268.html].
[27] Bioenergy in Germany: facts and figures, FNR- Central Coordinating Agency in the Area of Renewable Resources in Germany, 2019. https://mediathek.fnr.de/broschuren/fremdsprachige-publikationen/english-books/bioenergy-in-germany-facts-and-figures.html.
[28] S. Sahota, G. Shah, P. Ghosh, R. Kapoor, S. Sengupta, P. Singh, V. Vijay, A. Sahay, V.K. Vijay, I.S. Thakur, Review of trends in biogas upgradation technologies and future perspectives, Bioresour. Technol. Rep. 1 (2018) 79–88, https://doi.org/10.1016/j.biteb.2018.01.002.
[29] M. Beil, W. Beyrich, Biogas upgrading to biomethane. The Biogas Handbook, 2013, pp. 342–377.
[30] F. Bauer, T. Persson, C. Hulteberg, D. Tamm, Biogas upgrading - technology overview, comparison and perspectives for the future, Biofuels Bioprod. Biorefining 7 (5) (2013) 499–511, https://doi.org/10.1002/bbb.1423.
[31] M.A. Nemitallah, M.A. Habib, H.M. Badr, S.A. Said, A. Jamal, R. Ben-Mansour, E. M.A. Mokheimer, K. Mezghani, Oxy-fuel combustion technology: current status, applications, and trends, Int. J. Energy Res. 41 (12) (2017) 1670–1708, https://doi.org/10.1002/er.3722.
[32] R. Stanger, T. Wall, R. Spörl, M. Paneru, S. Grathwohl, M. Weidmann, G. Scheffknecht, D. McDonald, K. Myöhänen, J. Ritvanen, S. Rahiala, T. Hyppänen, J. Mletzko, A. Kather, S. Santos, Oxyfuel combustion for $CO_2$ capture in power plants, Int. J. Greenh. Gas Control. 40 (2015) 55–125, https://doi.org/10.1016/j.ijggc.2015.06.010.
[33] F. Carrasco-Maldonado, R. Spörl, K. Fleiger, V. Hoenig, J. Maier, G. Scheffknecht, Oxy-fuel combustion technology for cement production – State of the art research and technology development, Int. J. Greenh. Gas Control. 45 (2016) 189–199, https://doi.org/10.1016/j.ijggc.2015.12.014.
[34] M. Bailera, D.P. Hanak, P. Lisbona, L.M. Romeo, Techno-economic feasibility of power to gas–oxy-fuel boiler hybrid system under uncertainty, Int. J. Hydrogen Energy 44 (19) (2019) 9505–9516, https://doi.org/10.1016/j.ijhydene.2018.09.131.
[35] I. Ullah Khan, M. Hafiz Dzarfan Othman, H. Hashim, T. Matsuura, A.F. Ismail, M. Rezaei-DashtArzhandi, I. Wan Azelee, Biogas as a renewable energy fuel – a review of biogas upgrading, utilisation and storage, Energy Convers. Manage. 150 (2017) 277–294, https://doi.org/10.1016/j.enconman.2017.08.035.
[36] H.G. Hirschberg, Handbuch Verfahrenstechnik und Anlagenbau, Springer, Berlin Heidelberg, 1999.
[37] E.C. Carlson, Don't gamble with physical properties for simulations, Chem. Eng. Prog. 92 (10) (1996) 35–46.
[38] D.-Y. Peng, D.B. Robinson, A new two-constant equation of state, Ind. Eng. Chem. Fundam. 15 (1) (1976) 59–64, https://doi.org/10.1021/i160057a011.
[39] S. McAllister, et al., Fundamentals of combustion processes, Mech. Eng. Series (2011) 243–302.
[40] M. Springer, C. Hofmann, S.-A. Kao, H. Stoffels, Methanbetriebener Mildhybrid-Antriebsstrang, MTZ - Motortechnische Zeitschrift 80 (7-8) (2019) 44–51, https://doi.org/10.1007/s35146-019-0058-6.
[41] FNR, Leitfaden Biogas: Von der Gewinnung zur Nutzung; Bioenergie. Fachagentur für Nachwachsende Rohstoffe, 2016. https://mediathek.fnr.de/leitfaden-biogas.html.
[42] MAN Truck Bus AG: POWER Gas Engines for Power Generation, 2019 [Accessed 20.04.2020; https://www.engines.man.eu/man/media/content_medien/doc/global_engines/power/Power_Gas_EN_181016_web.pdf].
[43] P.R.U.S. Arachchige, M.C. Melaaen, Aspen plus simulation of $Co_2$ removal from coal and gas fired power plants, Energy Procedia 23 (2012) 391–399, https://doi.org/10.1016/j.egypro.2012.06.060.
[44] R. Turton, R.C. Bailie, W.B. Whiting, J.A. Schaeiwitz, B. Debangsu, Analysis, synthesis, and design of chemical processes, in: Prentice Hall International Series in the Physical and Chemical Engineering Sciences, 4. ed., intern. ed. ed., 1 vol, Pearson Education Intern., Upper Saddle River (N.J.), 2013. XXXV, 965.
[45] A. Otto, Chemische, verfahrenstechnische und ökonomische Bewertung von Kohlendioxid als Rohstoff in der chemischen Industrie, in: Schriften des Forschungszentrums Jülich. Reihe Energie und Umwelt / energy and environment, Vol. 268, Jülich: Forschungszentrum, Zentralbibliothek, 2015. VIII, 272 S.
[46] T. Kuramochi, A. Ramírez, W. Turkenburg, A. Faaij, Comparative assessment of CO2 capture technologies for carbon-intensive industrial processes, Prog. Energy Combust. Sci. 38 (1) (2012) 87–112, https://doi.org/10.1016/j.pecs.2011.05.001.
[47] S. Schemme, J.L. Breuer, M. Köller, S. Meschede, F. Walman, R.C. Samsun, R. Peters, D. Stolten, H2-based synthetic fuels: a techno-economic comparison of alcohol, ether and hydrocarbon production, Int. J. Hydrogen Energy 45 (8) (2020) 5395–5414. http://www.sciencedirect.com/science/article/pii/S0360319919318580.
[48] M. Bui, C.S. Adjiman, A. Bardow, E.J. Anthony, A. Boston, S. Brown, P.S. Fennell, S. Fuss, A. Galindo, L.A. Hackett, J.P. Hallett, H.J. Herzog, G. Jackson, J. Kemper, S. Krevor, G.C. Maitland, M. Matuszewski, I.S. Metcalfe, C. Petit, G. Puxty, J. Reimer, D.M. Reiner, E.S. Rubin, S.A. Scott, N. Shah, B. Smit, J.P.M. Trusler, P. Webley, J. Wilcox, N. Mac Dowell, Carbon capture and storage (CCS): the way forward, Energy Environ. Sci. 11 (5) (2018) 1062–1176.
[49] L. Eggemann, N. Escobar, R. Peters, P. Burauel, D. Stolten, Life cycle assessment of a small-scale methanol production system: a Power-to-Fuel strategy for biogas plants, J. Clean. Prod. 271 (2020).
[50] R. Böhm, R.M. Schaidhauf, B. Wytopil, J. Franke, Analyse der Marktaussichten von Biogasanlagen, Zeitschrift für Energiewirtschaft 42 (2) (2018) 167–176, https://doi.org/10.1007/s12398-018-0224-4.
[51] Gesetz für den Ausbau erneuerbarer Energien, (Erneurbare-Energien-Gesetz - EEG, 2014. https://www.bmwi.de/Redaktion/DE/Downloads/G/gesetz-fuer-den-ausbau-erneuerbarer-energien.html.
[52] M. Scheftelowitz, D. Thrän, Biomasse im EEG 2016 - Hintergrundpaier zur Situatiom der Bestandsanlagen in den verschiedenen Bundesländern, Deutsches Biomasseforschungszentrum, 2016. https://www.dbfz.de/fileadmin/user_upload/Referenzen/Statements/Hintergundpapier_Biomasse_EEG2016.pdf.